



OPEN Vapor flux induced by temperature gradient is responsible for providing liquid water to hypoliths

Giora J. Kidron¹✉, Rafael Kronenfeld², Bo Xiao^{3,4}, Abraham Starinsky¹, Christopher P. McKay⁵ & Dani Or^{6,7}✉

Commonly comprised of cyanobacteria, algae, bacteria and fungi, hypolithic communities inhabit the underside of cobblestones and pebbles in diverse desert biomes. Notwithstanding their abundance and widespread geographic distribution and their growth in the driest regions on Earth, the source of water supporting these communities remains puzzling. Adding to the puzzle is the presence of cyanobacteria that require liquid water for net photosynthesis. Here we report results from six-year monitoring in the Negev Desert (with average annual precipitation of ~90 mm) during which periodical measurements of the water content of cobblestone undersides were carried out. We show that while no effective wetting took place following direct rain, dew or fog, high vapor flux, induced by a sharp temperature gradient, took place from the wet subsurface soil after rain, resulting in wet-dry cycles and wetting of the cobblestone undersides. Up to 12 wet-dry cycles were recorded following a single rain event, which resulted in vapor condensation on the undersides of the cobblestones, with the daily wet phase lasting for several hours during daylight. This 'concealed mechanism' expands the distribution of photoautotrophic organisms into hostile regions where the abiotic conditions limit their growth, and provides the driving force for important evolutionary processes not yet fully explored.

Keywords Cobblestones, Cyanobacteria, Dew, Distillation, Fog, Lithobionts

Rendering a deep green tint to the ventral side (underside) of the surface of cobblestones, hypoliths consisting primarily of cyanobacteria and algae (photoautotrophs) and by heterotrophs (bacteria and fungi) are common in deserts^{1,2}. They abound below translucent quartz pebbles³, but are also found under opaque rock particles and partially embedded pebbles. Inhabiting the North American and the Australian deserts^{4,5}, the Gobi⁶, the Negev^{7,8}, the Namib^{9,10}, and the Atacama^{11–13}, hypoliths were reported to fix nitrogen^{14,15}, and to serve as important contributors of carbon in hyperarid regions where they may contribute 10–20% of the total carbon input¹⁶. The species composition of hypolithic communities is distinct from that of the adjacent soil^{1,17–19}. Moreover, although inhabiting the most hostile biomes, and being the only photoautotrophs in some of the most xeric loci within these hyperarid regions⁴, sequence-based identification reveals extremely diverse communities, comparable and even more diverse than those characterizing adjacent sky-facing lithic communities²⁰.

Sheltered from direct rain, and often decoupled from soil surfaces, the water source supporting hypolithic communities remains puzzling. This puzzle is accentuated by the fact that cyanobacteria globally predominate in these communities^{4,21}. Unlike eukaryotes that may perform net photosynthesis at RH ≥ 80%²², cyanobacteria require liquid water for growth^{22,23}. Despite this essential dependence on liquid water, they inhabit extreme hot (Atacama) and cold (the Dry Valleys in Antarctica) deserts where liquid water is extremely scarce.

While it was traditionally assumed that hypoliths benefit from rain^{18,24}, they were also thought to benefit from dew and fog^{7,11,18,25–27}. The scholarship has also suggested other potential water sources such as surface runoff^{28,29}, capillary wicking³⁰, and water trickling following rain, dew or fog³¹. Nevertheless, none of the above-

¹Institute of Earth Sciences, The Hebrew University of Jerusalem, Givat Ram Campus, Jerusalem 91904, Israel.

²Meteorological unit, Israel Meteorological Service, Kibbutz Sede Boqer 84993, Israel. ³Key Laboratory of Arable Land Conservation in North China, Ministry of Agriculture and Rural Affairs, College of Land Science and Technology, China Agricultural University, Beijing 100193, China. ⁴State Key Laboratory of Soil Erosion and Dryland Farming on the Loess Plateau, Institute of Soil and Water Conservation, Chinese Academy of Sciences and Ministry of Water Resources, Yangling 712100, Shaanxi, China. ⁵Space Science Division, Ames Research Center, National Aeronautics and Space Administration, Mountain View, CA, USA. ⁶Department of Environmental Systems Science, Swiss Federal Institute of Technology ETH, Universitätstrasse 16, Zürich CH-8092, Switzerland.

⁷Desert Research Institute, Division of Hydrologic Sciences, 2215 Raggio Parkway, Reno, NV 89512, USA. ✉email: kidron@mail.huji.ac.il; Dani.or@env.ethz.ch

mentioned mechanisms were substantiated by direct measurements. In contrast, high correlation was found with soil humidity > 95%, but surface wetting was not determined³². To date, no satisfactory mechanism has been proposed for wetting the undersides of cobblestones in hyperarid environments, particularly for conditions in which no direct contact exists between the hypolithic organisms and the soil.

In the Negev Highlands with a mean annual rainfall of ~ 90 mm and 200 dewy days a year³³, hypoliths (with *Chroococciopsis* sp. Predominating^{7,25}) are widespread. Hypoliths are also common in the southern Negev⁸ where mean annual rainfall is only ~ 30 mm and dew is scarce³⁴. Evidence suggests that the limited sky-view factor (SVF)³⁵ of the cobblestone underside would prevent nighttime substrate temperatures (T_s) from reaching the dew-point temperatures (T_d) required for atmospheric vapor condensation^{36,37}. Thus, the predominance of cyanobacteria in the hypolithic communities of the Negev, despite the high threshold of liquid water required for their net photosynthesis²³, represents a paradox requiring an explanatory mechanism.

Kidron et al.³⁸ reported observational evidence from the Negev that wet-dry cycles (WDCs) occur on the soil surface following medium and high-depth rain events (> 5 mm) during which vapor transport (from the wet soil) promotes vapor condensation on the cooler soil surface and in addition on aboveground substrates³⁹, explained by distillation (condensation resulting from vapor that stems from the wet soil). The onset of WDCs was attributed to large diurnal temperature gradients within the wet soil. We hypothesize that temperature-induced vapor flux (TIVF) can provide the necessary water source to support hypoliths and that by attaching thin (1 mm-thick) absorbing substrates such as cloths, the amount condensed on the cobble underside can be measured, similarly to the way such cloths were used to measure vapor condensation on the cobblestone tops³⁸.

Here we report results from field studies designed to test the TIVF hypothesis and evaluate the potential roles of alternate sources of water in wetting the underside surfaces of cobblestones (hereafter cobbles) using methods similar to those previously described^{38,39}. By preventing runoff and capillarity and by measuring the amount of water accumulating on velvet-like cloths and magnetized plastic sheets that were attached to the cobble underside, the amount of vapor reaching the cobble underside from the underlying soil was assessed (Fig. 1a). The occurrence of TIVF was also examined by measuring water and temperature with soil depth. For comparison, the amount of dew, fog and atmospheric vapor accumulating on the cobbles were also periodically measured by the cloths and magnetized plastic sheets (MPSs) that were attached to the top of the cobble during the dry season (Fig. 1b). As reference, we measured the amount of water (dewfall, distillation) via the cloth-plate method (CPM)⁴⁰, a cloth attached to 10 cm × 10 cm × 0.2 cm glass plates.

For quantitative calculations, we define the water threshold required for the predominant microorganisms (cyanobacteria) to perform net photosynthesis, which was found to be 0.1 mm²³, and which was also found to represent the minimum threshold that indicates liquid water²³.

The field experiments were conducted in the Negev Highlands for a period of six years (2014/15, 2015/16, 2017/18, 2019/20, 2021/22, 2022/23).

Results and discussion

Hypoliths were present on 86.7% of the hilltop cobbles, having chlorophyll *a* content of 18.3 (SD = 4.0) mg m⁻². Mean rain precipitation of ≥ 1 mm rain events during the study period was similar to the long-term mean (92.7 mm; Table S1). As shown in Table S1 most rainfall events were small (< 5 mm per event), with only 7 large events (> 20 mm) occurring during the experiment. Apart from a restricted area around the periphery of a cobble underside, rain did not commonly wet the underside of cobbles, and the amount of moisture found on the cloths following rain was ≤ 0.03 mm, ruling out the possibility of direct wetting by rain trickling. No wetting took place by dew or fog (Fig. 2). Also, no trickling was observed following dew or fog, explained by the sharp decrease in the amount of dew over the sides of the cobble with the increase in the substrate angle⁴¹.

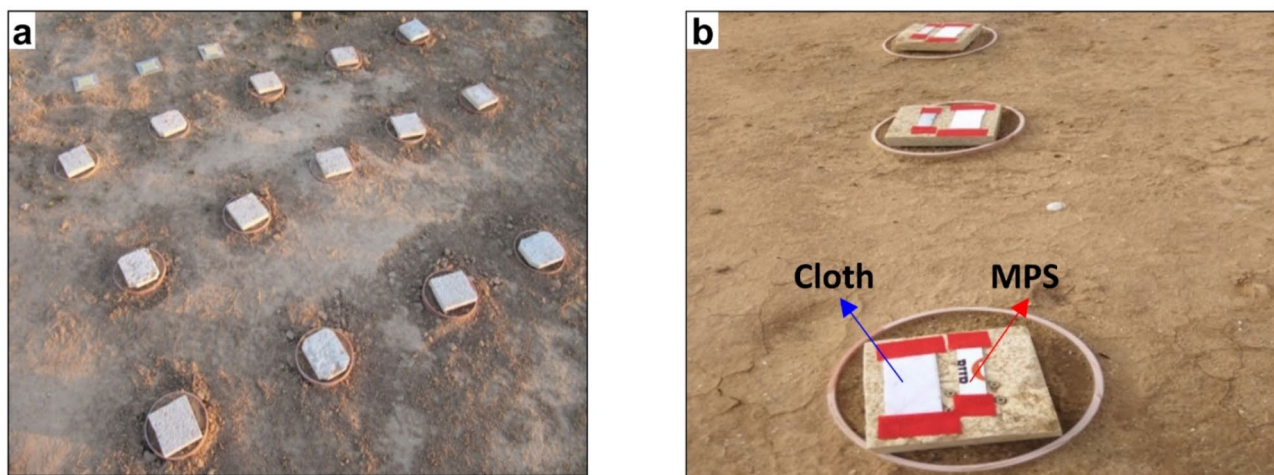


Fig. 1. Cobbles at the research site during the wet season during which cloths and MPSs are attached to the cobble undersides (a) and cloths and MPSs attached also to the top of the cobble during the dry season aiming to assess the effect of dew and fog on the water regime of the cobbles (b).

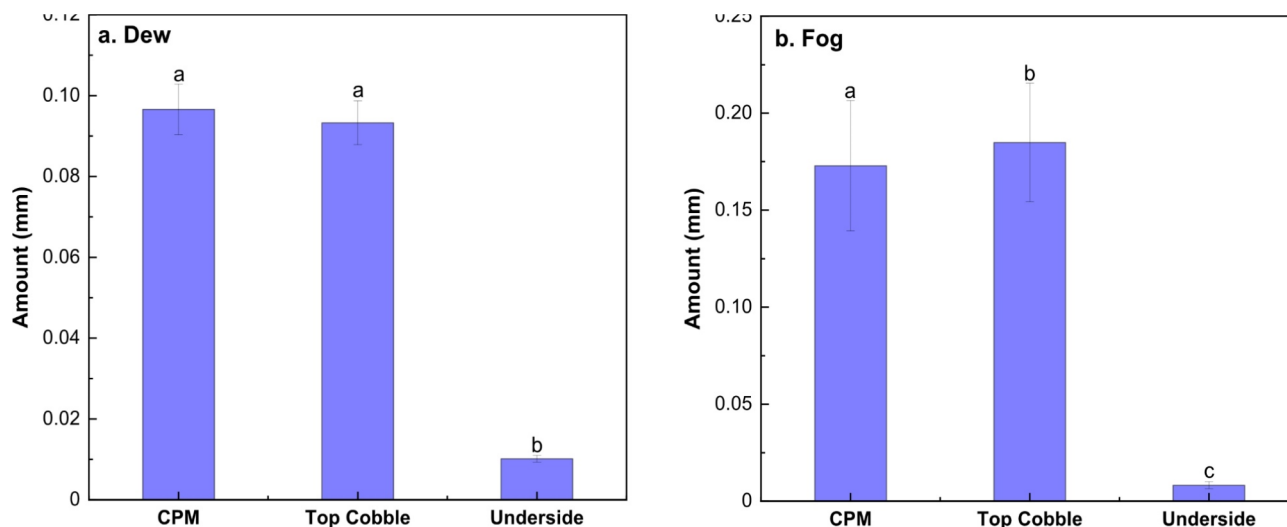


Fig. 2. Average amount of deposited dew ($N=62$) (a), and fog ($N=10$) (b) as measured by the cloth-plate method and with cloths attached to the top and underside of cobbles during the rainless dry season. Bars indicate one standard error. Different letters indicate significant differences ($P < 0.05$). The values are reported as equivalent depth of water per unit area (mm).

Figure 2 shows the average concomitant amount of atmosphere-driven non-rainfall water from dew ($N=62$) and fog ($N=10$), as periodically measured by the CPM and on the top and underside of the cobbles during the summers of 2016, 2019, 2020, 2021 and 2022. While relatively high amounts of dew and fog (~0.10–0.20 mm) were obtained on the top of the cobbles and on the CPM during the non-rainy period, only minute values (≤ 0.02 mm) were recorded on the cobble undersides.

During the morning and noon hours after a rain event, WDCs were periodically monitored (days during which monitoring took place are indicated in Table S1). WDCs were observed for a week or more following a rain event (in accordance with rain depth; see below), during which a wet soil surface was visible during the morning. Commonly and except for cloudy days, surface desiccation took place during midday, but rewetting of the soil surface was observed again during the following morning. These WDCs, which were previously described in desert surfaces^{38,42–45}, were primarily explained by vapor transport^{42–51}. WDCs were also noted on the open surfaces of the Negev following rain events that wetted the upper several centimeters of the soil³⁸. As verified by temperature and moisture measurements, WDCs also took place on the cobble undersides.

Temperature distributions as measured during 16–18 March, 2023 (following the 9.1 mm rain event of 14 March, 2023 and during 14–16 April, 2023 (following the 24.4 mm rain event of 10–12 April, 2023) on the cobble undersides are shown in Fig. 3a₁ and a₂, respectively. These measurements show consistent differences with a clear gradient. The warm-to-cold gradient from the subsurface to the surface during the late night and the early morning and an opposite gradient during midday support the occurrence of vapor movement, as found in previous experiments^{48,52}. For example, during the 9.1 mm rain event of 14 March, 2023 the minimum temperature measured on the underside of the cobble was 5.0 °C lower than at 9 cm below surface, and 2.3 °C and 1.6 °C lower than at 3 cm and 1 cm below surface, respectively. These thermal gradients are larger than the required thermal gradient of 0.5 °C cm⁻¹ reported by Cary⁵² to support substantial vapor flow. The vapor transport and condensation were also reflected by clear moisture cycles within the soil underlying the cobbles.

The water dynamics in the subsurface soil as recorded under the cobbles are shown in Fig. 3b₁ and b₂. These figures show clear diurnal cycles. For instance, an increase in water content near the surface (at 2.0 cm depth) took place during the early morning while an increase in water content at 4.5 cm depth (with a concomitant decrease at 2.0 cm) took place during midday. The increase in water content at 2.0 cm below surface during the early morning hours lends support to the proposed TIVF hypothesis during which vapor from the subsurface condenses on the cobble undersides.

High values of water content on the underside of the cobbles were indeed observed following rain events (Fig. 4a,b), with both substrates, cloths and MPSs, yielding comparable results (Fig. S1). As depicted in Fig. 5, these amounts were as high as 0.5 mm and lasted for up to 7 h (for instance during 12 January, 2015). These values were higher than the commonly recorded dew values on the top of cobbles following atmosphere-driven non-rainfall water, which seldom exceeded 0.25 mm (Fig. 2).

Following winter rain events, WDCs may commonly last for a week but may even last for 12 days after a large rain event during favorable (cool) temperature conditions. This was evident following the high-depth rain event of 29.4 mm of 7–11 January, 2015 (and additional 2.1 mm that fell during 16 January, 2015) (Fig. 5). The results in Fig. 5 highlight the increased accumulation of water during the morning hours followed by a sharp decrease (due to the cobble warming by radiation) during the rest of the day. As can be noted in Fig. 5 and following

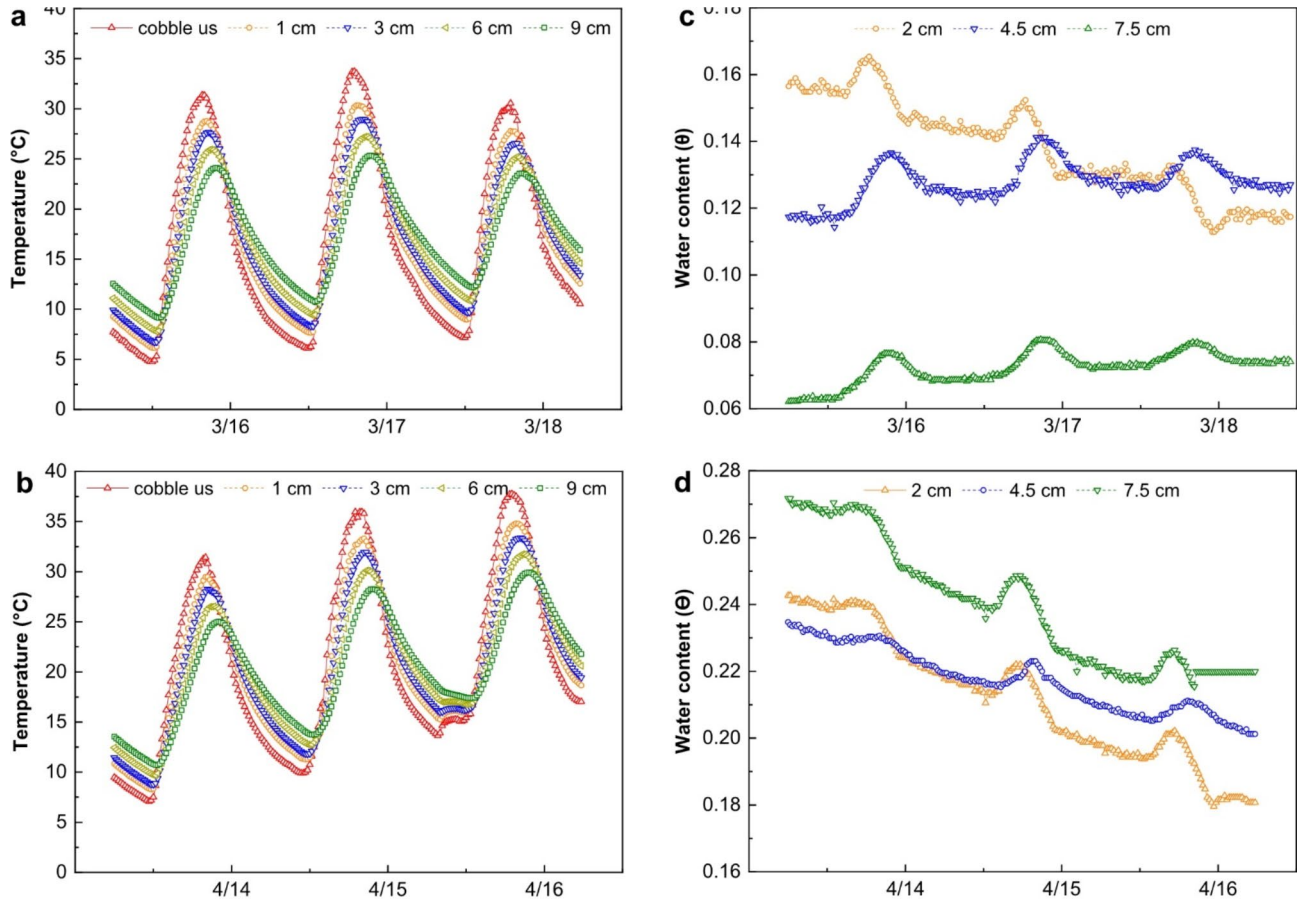


Fig. 3. Daily temperatures as measured on the underside of the cobble (cobble us) and at 1, 3, 6, 9 cm below surface following the 9.1 mm rain event of 14 March, 2023 (DOY 73 in Table S1) (a₁) and the 24.4 mm rain event of 10–12 April, 2023 (DOY 100–102 in Table S1) (a₂), and the water content at 2.0, 4.5 and 7.5 cm below cobbles following the 9.1 mm rain event of 14 March, 2023 (DOY 73 in Table S1) (b₁), and water content at 2.0, and 4.5 cm below cobbles following the 24.4 mm rain event of 10–12 April, 2023 (DOY 100–102 in Table S1) (b₂).

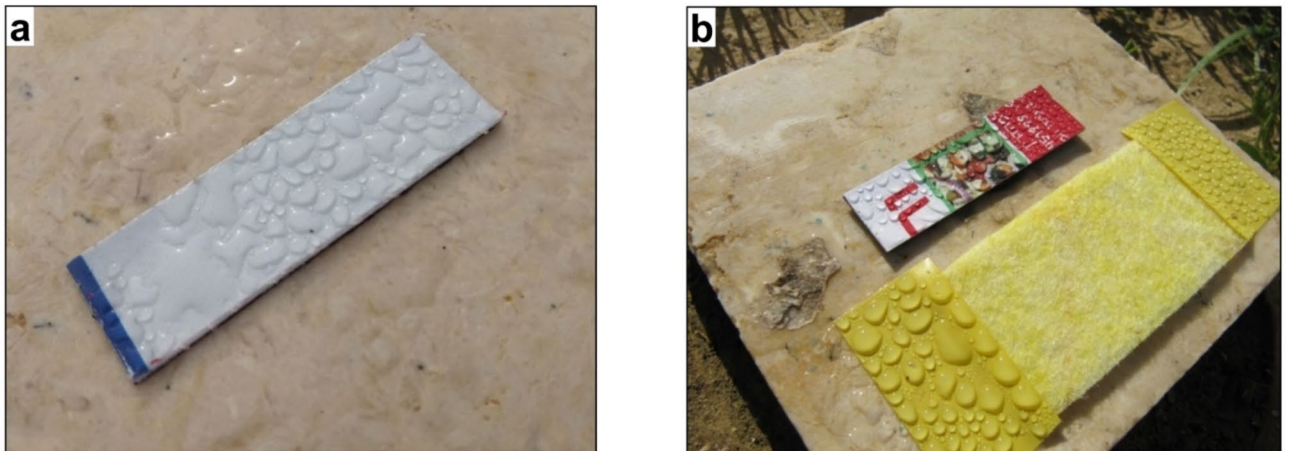


Fig. 4. Vapor condensation on the underside of a cobble on a MPS (0.23 mm as measured at 09:00 on 13 January, 2015) following the rain event of 7–11 January, 2015 (a), and 0.20 mm as obtained on a MPS and a cloth (bottom) on 7 January, 2022 following the rain event of 14.8 mm during 1–3 January, 2022 (b).

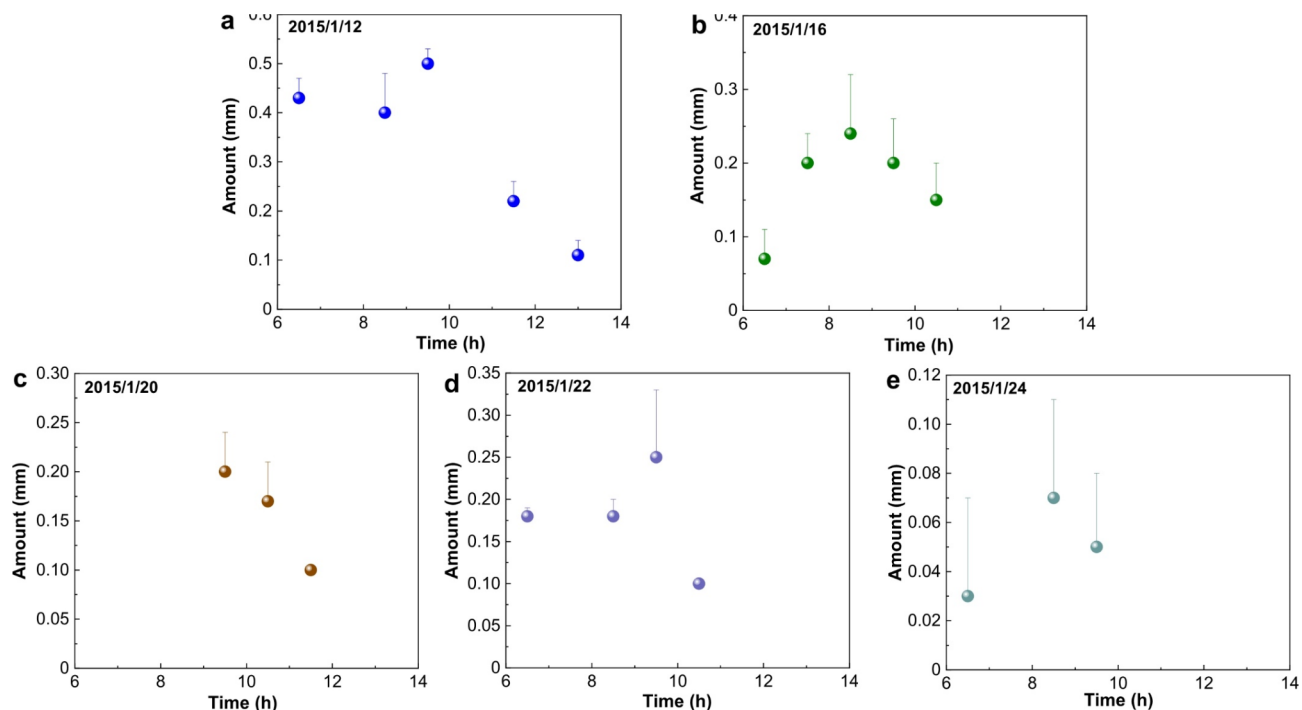


Fig. 5. WDCs as measured during 5 days using MPS following the 29.4 mm that fell during 7–11 January, 2015 (DOY 7–11 in Table S1), and an additional 2.1 mm that fell during 16 January, 2015 (DOY 16 in Table S1). Bars represent one standard error.

other rain events, each of the cycles becomes shorter with the elapsed time since the rainfall event – an expected outcome following soil water loss with time.

The extent (i.e., number of cycles and the length of the daily wet phase of each cycle) of the WDCs also depends upon the ambient temperatures. The lower the nocturnal air temperature, the sooner the vapor condensation³⁷ and the higher the maximum water content on the cobble undersides (Fig. S2). Also, the lower the temperature, the higher the number of the WDCs. And thus, in comparison to rainstorms during the warm spring days, the cool winter rain events result in a longer wet phase during each WDC and a substantially higher number of WDCs. This can be clearly seen once winter and spring rain events of similar magnitudes are compared. In comparison to 7 WDCs monitored following the 14.8 mm winter rain event of 1–3 January, 2022 only 4 WDCs were monitored following the 15.0 mm spring rain event of 12–13 April, 2016 (Fig. 6). Indeed, while the average maximum air temperature during the week that followed the 1–3 January, 2022 event was 17.8 °C, it was 28.8 °C for the week following the 12–13 April, 2016 rain event. Also, as can be seen in Fig. 3a, whereas the soil temperatures at 1 cm depth below the cobble rose during the three days following the 14 March, 2023 rain event by 2.8 °C, they rose by 7.8 °C during the three days following the rain event of 10–12 April, 2023.

The temperature effect was also clearly demonstrated once the wetness duration under the cobbles was calculated. Figure 7 shows the calculations for five pairs of winter (19–20 February, 2020; 8 February, 2023; 1–3 January, 2022; 7–11, January, 2015; 24–25 February, 2020) and spring (10–12 April, 2015; 14 March, 2023; 12–13 April, 2016; 12–14 March, 2020; 10–12 April, 2023) rain events of comparable magnitudes. While average daylight wetness duration for a winter event was 26.1 h (SD = 5.7), it was only 10.6 h (SD = 4.3) for the spring event. Wetness duration following the winter events lasted ~2.5 fold longer in comparison to the rain events during the spring.

A schematic model depicting the WDCs and the subsequent wetting of the cobble undersides is shown in Fig. 8. Unlike dew and fog that provide water to the cobble tops, TIVF provides water to the hypolithic community. Whereas distillation serves as the source of water to the hypolithic community, non-rainfall water and distillation provide water to lichens residing on the sky-facing surfaces of the cobbles³⁹.

One should however note that through shading, the cobbles impede surface cooling during the night but at the same time, by facilitating lower daytime temperatures (Fig. 3), they impede daytime evaporation. This may explain the observation that hypolithic communities were commonly found on cobbles > 10–11 cm in diameter²⁸. The impediment of daytime vapor loss may also explain the occurrence of hypoliths on the underside of partially embedded cobbles³, supported by field observations noting that the undersides of these cobbles were wet⁵³.

Interestingly however, as can be noted in Fig. 5, the maximal water content on the cobble underside was commonly measured only 2–3 h after sunrise. Such a process is supported by the pattern that described the increase in water drops during condensation as observed on the MPSS, i.e., individual semi-circular drops with clear boundaries typical of vapor condensation³⁷ (Fig. 4). It is suggested that as the soil is warmed up by the first

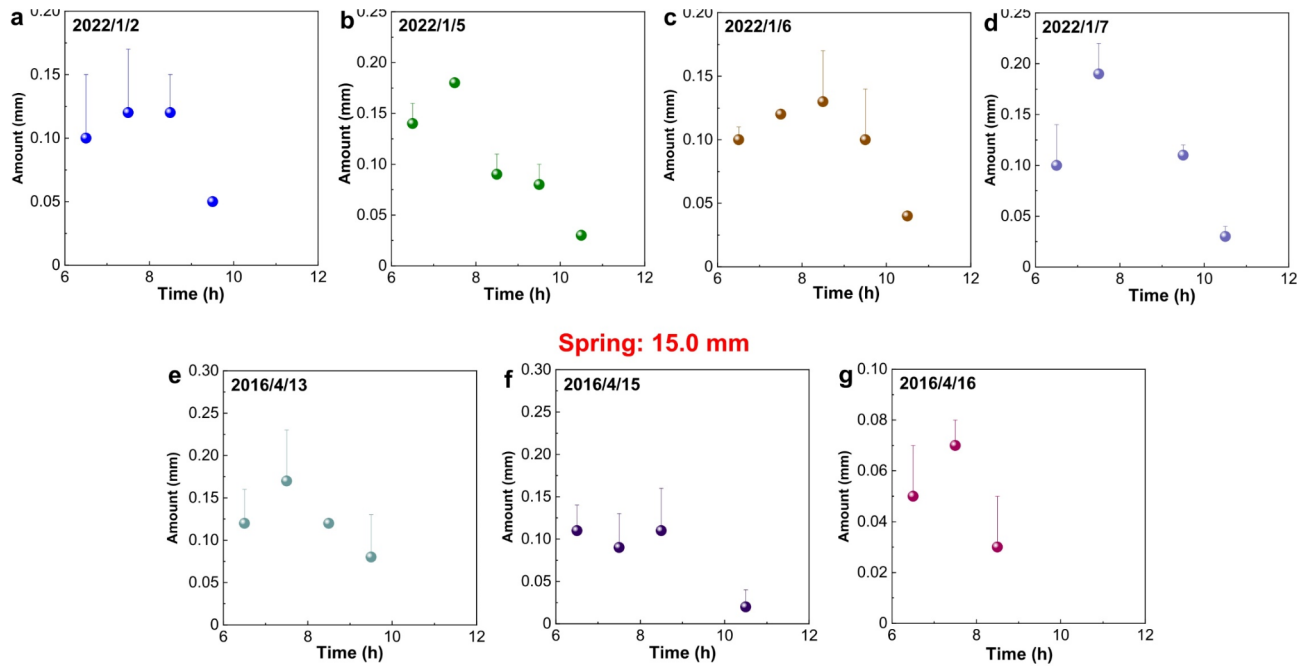


Fig. 6. A comparison between a 14.8 mm rain event that took place during the winter (1–3 January, 2022, i.e., DOY 1–3 in Table S1) (a) and a 15.0 mm rain event that took place during the spring (12–13 April, 2016, i.e., DOY 102–103 in Table S1) (b). Bars represent one SE.

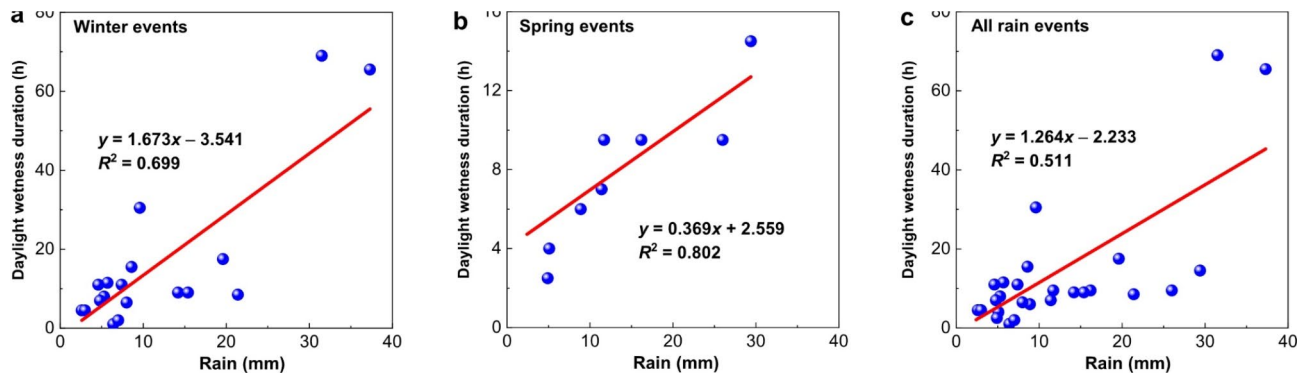


Fig. 7. The relationships between the rain depth and the daylight time duration during which > 0.1 mm was recorded on the underside of the cobbles during five pairs of rain events with comparable magnitudes during the winter (19–20 February, 2020; 8 February, 2023; 1–3 January, 2022; 7–11 January, 2015; 24–25 February, 2020) (a), the spring (10–12 April, 2015; 14 March, 2023; 12–13 April, 2016; 12–14 March, 2020; 10–12 April, 2023) (b) and during both seasons (c).

sun rays soon after sunrise, an enhanced vapor flux from the subsurface to the cobble underside takes place, apparently stemming from increased turbulence within the soil pores. It is worth noting that a similar process during which enhanced condensation of atmospheric vapor took place after sunrise was also reported to take place on the top of lithobiont-inhabiting cobbles⁵⁴.

Based on the rain distribution during 1990–2020 and the magnitude of the WDCs during winter and spring, we calculated the annual wetness duration of the hypolithic community in the Negev (Table 1). On average, 13 large (> 30 mm), 45 medium (10–20 mm) and 168 small (1–5 mm) rain events characterize the rainy period (data obtained from the IMS meteorological station in Sede Boqer; https://ims.gov.il/he/data_gov). On average, winter and spring rain events provide 76.4 h, and 15.1 h, of daylight wetness duration per year, respectively, totaling 91.5 h. However, when calculating the time during which prolonged rainy days (that lasted for 2–4 days) took place (during which no field measurements were conducted by us), total wetness duration calculated for the undersides of the cobbles is 124.7 h (Table 1).

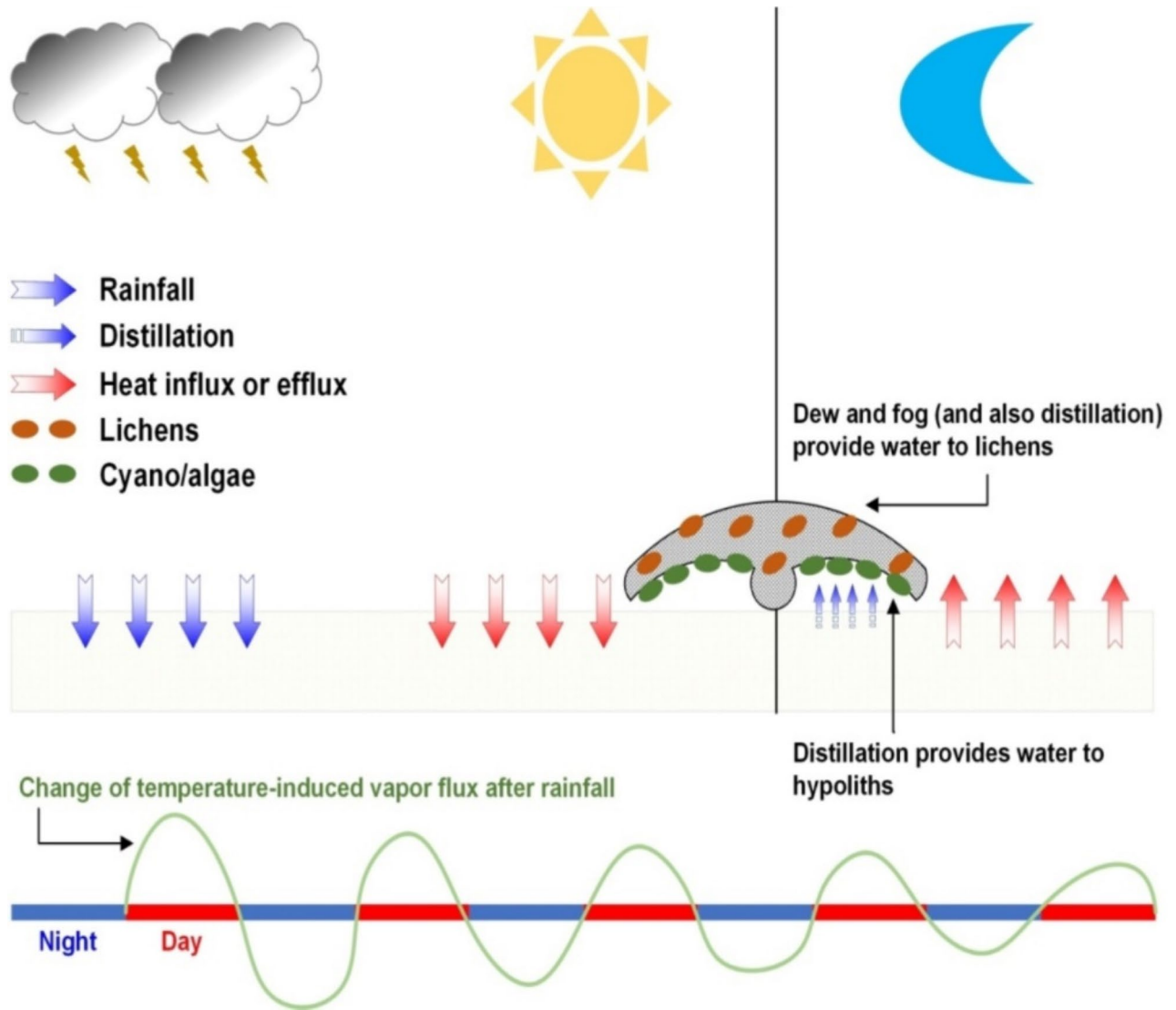


Fig. 8. A schematic presentation of the suggested mechanism. Following rain, heat influx (during the day) and efflux (during the night) results in water evaporation and water transport to the soil subsurface during the day and water transport to the soil surface and the underside of cobbles during the night and the very early morning hours. Whereas lichens on the sky-facing cobbles in the Negev also benefit from dew and fog, TIVF-driven distillation is the only source of water available to the hypoliths. Note that the magnitude of the cycles (bottom drawing) is getting smaller with time until ceased.

One may however note that the actual value may be even higher. In comparison to cobbles that lie on the ground, our cobbles were kept 2 mm above ground, being therefore subjected to enhanced evaporation by the morning wind⁵⁴. Additionally, since cyanobacteria commonly excrete exopolymeric substances that may retain water for an extended time⁵⁵, one may conclude that our calculations may be conservative and the cyanobacteria activity may be longer than that calculated by us. Also, since the photoautotrophic eukaryotes such as green algae may perform net photosynthesis already at relative humidity of 80%⁵⁶, which corresponds to 0.05 mm⁵⁶, the overall photosynthetic period of activity of the entire hypolithic community may be longer than that estimated by us.

Wetness duration as calculated by us on the cobbles undersides is higher than the wetness duration calculated for lithic cyanobacteria in this region (90.6 h)⁵⁷. Since daylight wetness duration rather than the amount of water determines the photosynthetic period of activity and subsequently the lithobiont biomass^{57,58}, it may explain the higher chlorophyll content of the hypoliths (18.3 mg m⁻²), in comparison to the lithic cyanobacteria covering the top (sky-facing) surface rocks (11.7 mg m⁻²)⁵⁹. However, the higher chlorophyll content of the hypolithic community may be also explained by their shaded position, which provides protection from the harmful UV, attesting to the favorable conditions of the hypolithic habitat.

In comparison to coastal deserts that may also benefit from dew or fog and are therefore characterized by exceptionally high-biomass lithobionts^{59,60}, most deserts lie inland where rain provides their main (if not the sole) source of water. With the underside of cobbles serving as a local water harvesting surface, hypoliths thus inhabit

Rain event (mm)	Total events for 30 years		Events per year		Wetness duration (h)	
	Winter	Spring	Winter	Spring	Winter	Spring
1–5	133	35	4.43	1.17	11.6	5.7
5–10	56	14	1.87	0.47	17.8	1.1
10–20	29	16	0.97	0.53	20.4	4.5
20–30	9	3	0.30	0.10	11.0	2.9
> 30	11	2	0.37	0.07	19.1	5.6
Days with continuous rain ¹	3.9	0.8	3.9	0.8	27.3	2.4
Total					107.1	17.6
Total for the year						124.7

Table 1. Calculating the wetness duration during which the amount of water at the hypolithic community was > 0.1 mm. Calculations were based on the number of rain events with 1–5, 5–10, 10–20, 20–30 mm and > 30 mm that fell at Sede Boqer during the last 30 years (1990–2020) during the winter (November until March 15th) and spring (March 16th until end of May) months. ¹Calculating rainy days during which measurements were not carried out, but TIVF took place. We registered the amount of these days for each year during 1990–2020. We calculated an average activity of 7 h and 3 h for each of these rainy days during winter and spring, respectively.

the most favorable habitat in these hyperarid regions. With microorganisms being capable of long dormancy (dozens of years) under limited water supply⁶¹, providing that the hazardous effect of UV radiation is minimal¹², the negligible UV radiation on the cobble underside exerts extra advantage to the hypolithic community²⁹. Hypoliths may thus serve as a useful indicator for decade-long rainfall distribution and magnitude. This may explain their presence in the most extreme hot deserts (e.g. the Namib⁶¹ and the Atacama⁶²) even under conditions of year-long paucity of rain.

Because cyanobacteria are also capable of fixing nitrogen^{5,14}, the hypolithic habitat may be regarded as the least nutrient-limited habitat in hyperarid environments¹⁵. In hyperarid regions the hypolithic habitats are further regarded as the ‘only significant source of primary production... (acting) as reservoirs for terrestrial biota’ and as ‘the last refuge for life’²⁰. The enigma of the apparent contradiction between the high amount of water required by cyanobacteria and their presence in the most arid regions on Earth brought Pointing et al.²⁰ to suggest that an alternative model should be proposed in regard to their water requirements. This apparent paradox is however explained by the above-mentioned mechanism. This ‘concealed mechanism’ may explain the expanded distribution of photoautotrophs to areas where all other surfaces lack photoautotrophs⁴, may explain the very high diversity of the hypolithic community in comparison to sky-facing substrates²⁰, and the fact that the hypolithic habitat can therefore be regarded as one of the most mesic habitats within the most extreme deserts on Earth.

Research site and methodology

The research site is located in a loessial flat valley, Sede Zin, near Kibbutz Sede Boqer in the Negev Highlands, 480 m above MSL (34°23'E, 30°56'N). Long-term annual precipitation is 80–100 mm⁶³. Precipitation occurs in the winter months, between November and April. The average annual dew and fog formation is ~ 33 mm, with ~ 200 dewy and foggy days per year, during which the late summer and fall are particularly dewy³³. Average daily temperature is 17.9 °C; it is 24.7 °C during the hottest month of July and 9.3 °C during the coldest month of January⁶⁴. The annual potential evaporation is ~ 2600 mm⁶⁵.

Sede Zin borders 50–70 m-high limestone hills, with abundant cobbles that are covered by endolithic and epilithic lichens^{25,39}. These cobbles are also commonly inhabited by cyanobacteria-dominated hypoliths. For the evaluation of the hypolith frequency and their chlorophyll content, we conducted a survey during October, 2016. We randomly examined 60 cobbles from two hilltops (30 cobbles from each hilltop) and demarcated the boundaries of the visible patches (clearly noted by their deep green color) of the hypoliths. Hypoliths were present on 86.7% of the cobbles. Out of these cobbles, 20 cobbles were randomly chosen and the surface of 1 cm × 1 cm, randomly taken from each boundary limit was scrapped (using a sharp sterilized) blade) to a depth of ~ 5 mm for chlorophyll measurements. Chlorophyll was extracted by 5 mL of hot methanol (70°C, 20 min) in the presence of MgCO₃ (0.1% w/v) in sealed test tubes and assayed according to Wetzel and Weslake⁶⁶ using the equation:

$$\text{CHLa (mgL}^{-1}\text{cm}^{-2}\text{)} = (A_{665} - A_{645}) \times 13.9 \times 5. \quad (1)$$

To evaluate the capability of the different sources of water, rain, dew, fog and distillation to wet the underside surface of cobbles, measurements were conducted in our research site. For this end, we used fifteen 10 cm × 10 cm × 2–3 cm cobbles (3 rows of 5 cobbles each) that were carefully cut from the same slab to minimize possible differences in their structural, textural and physicochemical properties (Fig. 1a). Each cobble was laid within a 15 cm-diameter and 5 cm-high ring that protruded 1 cm-above ground aiming to prevent runoff entry into the underside of the cobble. While serving to impede runoff from the vicinity into the cobble underside, previous

measurements ruled out the possibility that the ring may have contributed water to the cobble underside, or affected the evaporation rate within the ring.

All cobbles were put on four 2 mm-diameter wooden sticks, keeping the cobbles ~2 mm above ground to prevent direct contact with the soil and therefore water capillarity. This also allowed us to weigh the amount of water that accumulates on depositional substrates (see below) attached to the cobble underside. One should note that the air gap may not have entirely mimicked the natural conditions as it may increase the evaporation induced by the morning wind, thus reducing the amount of water on the cobble underside. Our values may therefore be conservative as they may reflect minimum values implying that the actual water accumulating on the cobble underside may be even larger than those measured by us.

For the measurements of the water that accumulates on the cobble substrate, cloths and magnetized plastic sheets were used. Strips of 6 cm × 3 cm × 0.1 cm velvet-like PVA microfiber porous cloths (Vileda, Germany) were attached to the underside of the cobbles (using tapes) in order to evaluate the accumulated amounts. In addition, and in order to allow us to also visibly observe the diel distribution of the water, 6 cm × 1.5 cm × 0.05 cm magnetized plastic sheets (MPSs) were also periodically attached to the undersides of the cobbles (Fig. 1b). The attachment of each MPS to the underside of the cobble was done via a 0.5 cm-thick, 1.2 cm-diameter magnet that was inserted into a hole of similar dimensions (drilled to the center of the underside of each cobble), so that the MPS was kept flat with the underside surface of the cobble. Each magnet kept the MPS tightly to the cobble underside. By randomly collecting cloths and MPSs from one cobble from each row, we were able to complete up to five rounds of sample collections within a single morning, each containing 3 samples of cloths and MPSs. Cloths and MPSs were also attached to the top of the cobbles during the dewy and non-rainy period (late summer and fall). We assumed that while sampling of the cloths during the dewy season will allow us to assess the potentiality of dew and fog to wet the underside of the cobble, sampling followed rain events will allow us to assess whether the cloths were wetted by direct rain (once the collection of the cloths is carried out immediately following the cessation of the rain) or by distillation stemming from TIVF that may take place during WDCs after rain events.

The wetness duration was calculated by constructing a daily graph of evaporation (water amounts versus time of collection), based on the measured values and in line with the pattern that characterize dew⁵⁴ and rain⁶⁷ evaporation. Missing data were filled by extrapolation.

For reference, the cloth-plate method (CPM) was used. It consists of 6 cm × 6 cm × 0.1 cm velvet-like cloth that is attached to the center of a 10 cm × 10 cm × 0.2 cm glass plate, glued in turn to a 10 cm × 10 cm × 0.5 cm plywood plate that served to provide an identical base⁴⁰. During the current research a threshold of 0.1 mm, which is required by the cyanobacteria to perform net photosynthesis served to evaluate the annual estimated activity of the hypolithic community.

The cloths and MPSs were attached to the cobbles in the late afternoon and collected during the following morning. Each cloth and each MPS was separately placed into a glass flask that was immediately sealed. Following a rain event, the cloths and MPSs were collected in 1–2 h intervals throughout the morning and noon. To avoid cloth and MPS moistening by direct rain, the cloth and the MPS collection commonly commenced one day after the cessation of the rain. For calculating the water amount, the amount was divided by the surface area in accordance with the equation:

$$WC = (W_{\text{wet}} - W_{\text{dry}}) / (\rho A) \times 10, \quad (2)$$

where WC is the amount of water content in millimeters, W_{wet} and W_{dry} are the wet and dry weight of the cloths in grams, respectively, ρ is the density of water at given temperature in g cm^{-3} and A is the surface area in cm^2 .

In order to study the daily dynamics of the WDCs and TIVF, a pair of calibrated Hobo moisture sensors (S-SMx-M005 Soil Moisture Smart Sensor) connected to Hobo H21-USB Micro Station (Onset Computer Corporation, MA, USA) was installed during February 2023 at 2.0 cm, 4.5 cm and 7.5 cm depth under the cobbles. Temperatures were measured with a pair of calibrated (± 0.05 °C) 3 cm-long and 0.5 cm-diameter TMC6-HD thermistors (Onset Computer Corporation, MA, USA), inserted at 1, 3, 6 and 9 cm below surface and tightly attached to the cobble undersides. The temperature sensors were connected to U-12 Hobo data loggers (Onset Computer Corporation, MA, USA). All readings were carried out and saved in 20 min intervals.

Data availability

Data that support the findings was uploaded at Zenodo and can be found at: Giora Kidron. Zenodo. <https://doi.org/10.5281/zenodo.10864503>.

Received: 23 March 2024; Accepted: 18 September 2024

Published online: 04 October 2024

References

1. Wong, F. K. Y. et al. Hypolithic microbial community of quartz pavement in the high-altitude tundra of central Tibet. *Microb. Ecol.* **60**, 730–739. <https://doi.org/10.1007/s00248-010-9653-2> (2010).
2. Stomeo, F. et al. Hypolithic and soil microbial community assembly along an aridity gradient in the Namib Desert. *Extremophiles* **17**, 329–337. <https://doi.org/10.1007/s00792-013-0519-7> (2013).
3. Schlesinger, W. H. et al. Community composition and photosynthesis by photoautotrophs under quartz pebbles, southern Mojave Desert. *Ecology* **84**, 3222–3231. <https://doi.org/10.1890/02-0549> (2003).
4. Chan, Y. et al. Hypolithic microbial communities: Between a rock and a hard place. *Environ. Microbiol.* **14**, 2272–2282. <https://doi.org/10.1111.1462-2920.2012.02821.x> (2012).
5. Lacap-Bugler, D. C. et al. Global diversity of desert hypolithic cyanobacteria. *Front. Microbiol.* **8**, 867. <https://doi.org/10.3389/fmicb.2017.00867> (2017).

6. Wu, M. H. et al. Seasonal variation of hypolithic microbiomes in the Gobi Desert. *Microb. Ecol.* **85**, 1382–1395. <https://doi.org/10.1007/s00248-022-02043-3> (2023).
7. Berner, T. & Evenari, M. The influence of temperature and light penetration on the abundance of the hypolithic algae in the Negev Desert of Israel. *Oecologia* **33**, 255–260. <https://doi.org/10.1007/BF00344852> (1978).
8. McKay, C. P. Water sources for cyanobacteria below desert rocks in the Negev Desert determined by conductivity. *Glob. Ecol. Conserv.* **6**, 145–151. <https://doi.org/10.1016/j.gecco.2016.02.010> (2016).
9. Makhalanyane, T. P. et al. Evidence of species recruitment and development of hot desert hypolithic communities. *Environ. Microbiol. Rep.* **5**, 210–224. <https://doi.org/10.1111/1758-2229.12003> (2013).
10. Cowan, D. A. et al. Microbiomics of the Namib Desert habitats. *Extremophiles* **24**, 17–29. <https://doi.org/10.1007/s00792-019-01122-7> (2020).
11. McKay, C. P. et al. Temperature and moisture conditions for life in the extreme arid region of the Atacama Desert: Four years of observations including the El Niño of 1997–1998. *Astrobiology* **3**, 393–406. <https://doi.org/10.1089/153110703769016460> (2003).
12. Cockell, C. S., McKay, C. P., Warren-Rhodes, K. & Horneck, C. Ultraviolet radiation-induced limitation to epilithic microbial growth in arid deserts—Dosimetric experiments in the hyperarid core of the Atacama Desert. *J. Photochem. Photobiol. B Biol.* **90**, 79–87. <https://doi.org/10.1016/j.jphotobiol.2007.11.009> (2008).
13. Jung, P. et al. Water availability shapes edaphic and lithic cyanobacterial communities in the Atacama Desert. *J. Phycol.* **55**, 1306–1318. <https://doi.org/10.1111/jpy.12908> (2019).
14. Cowan, D. A. et al. Hypolithic communities: important nitrogen sources in Antarctic desert soils. *Environ. Microbiol. Rep.* **3**, 581–586. <https://doi.org/10.1111/j.1758-2229.2011.00266.x> (2011).
15. Ramond, J. B., Woodborne, S., Hall, G., Seely, M. & Cowan, D. A. Namib Desert primary productivity is driven by cryptic microbial community N-fixation. *Sci. Rep.* **8**, 6921. <https://doi.org/10.1038/s41598-018-25078-4> (2018).
16. Monus, B. D., Nghalipo, E. N., Marufu, V. J., Garcia-Pichel, F. & Throop, H. L. Contributions of hypolithic communities to surface soil organic carbon across a hyperarid-to-arid climate gradient. *Geoderma* **433**, 116428. <https://doi.org/10.1016/j.geoderma.2023.116428> (2023).
17. Smith, B. J., Warke, P. A. & Moses, C. A. Limestone weathering in contemporary arid environments: A case study from southern Tunisia. *Earth Surf. Process. Landf.* **25**, 1343–1354. [https://doi.org/10.1002/1096-9837\(200011\)25:12%3C1343::AID-ESPI42%3E3.0.CO;2-2](https://doi.org/10.1002/1096-9837(200011)25:12%3C1343::AID-ESPI42%3E3.0.CO;2-2) (2000).
18. Warren-Rhodes, K. A. et al. Hypolithic cyanobacteria, dry limit of photosynthesis, and microbial ecology in the hyperarid Atacama Desert. *Microb. Ecol.* **52**, 389–398. <https://doi.org/10.1007/s00248-006-9055-7> (2006).
19. Fisher, K., Jefferson, J. S. & Vaishampayan, P. Bacterial communities of Mojave Desert biological soil crusts are shaped by dominant phototrophs and the presence of hypolithic niches. *Front. Ecol. Evol.* **7**, 518. <https://doi.org/10.3389/fevo.2010.00518> (2020).
20. Pointing, S. B. et al. Highly specialized microbial diversity in hyper-arid polar desert. *PNAS* **106**, 19964–19969. <https://doi.org/10.1073/pnas.0908274106> (2009).
21. Caruso, T. et al. Stochastic and deterministic processes interact in the assembly of desert microbial communities on a global scale. *ISME J.* **5**, 10406–11413. <https://doi.org/10.1038/ismej.2011.21> (2011).
22. Lange, O. L., Kilian, E. & Ziegler, H. Water vapor uptake and photosynthesis of lichens: Performance differences in species with green and blue-green algae as phycobionts. *Oecologia* **71**, 104–110. <https://doi.org/10.1007/BF00377327> (1986).
23. Lange, O. L. et al. Taxonomic composition and photosynthetic characteristics of the biological soil crusts covering sand dunes in the Western Negev Desert. *Func. Ecol.* **6**, 519–527. <https://doi.org/10.2307/2390048> (1992).
24. Warren-Rhodes, K. A., Rohdes, K. L., Liu, S., Zhou, P. & McKay, C. P. Nanoclimate environment of cyanobacterial communities in China's hot and cold hyperarid deserts. *J. Geophys. Res.* **112**, G01016. <https://doi.org/10.1029/2006JG000260> (2007).
25. Friedmann, E. I. & Galun, M. Desert algae, lichens and fungi. In: *Desert Biology II* (ed. Brown, G.W.), 165–212 (Academic Press, New York, 1974) (1974).
26. Davila, A. F. et al. Facilitation of endolithic microbial survival in the hyperarid core of the Atacama Desert by mineral deliquescence. *J. Geophys. Res.* **113**, G1. <https://doi.org/10.1029/2007JG000561> (2008).
27. Azúa-Bustos, A. et al. Hypolithic cyanobacteria supported mainly by fog in the coastal range of the Atacama Desert. *Microb. Ecol.* **61**, 568–581. <https://doi.org/10.1007/s00248-010-9784-5> (2011).
28. Warren-Rhodes, K. A. et al. Cyanobacterial ecology across environmental gradients and spatial scales in China's hot and cold deserts. *FEMS Microbiol. Ecol.* **61**, 470–482. <https://doi.org/10.1111/j.1574-6941.2007.00351.x> (2007).
29. Pointing, S. B. Hypolithic communities. In: *Biological Soil Crusts: An Organizing Principle in Drylands* (eds Weber, B. et al.) 199–213 (Springer, 199–213. https://doi.org/10.1007/978-3-3198-30214-0_11 (2016).
30. Gómez-Silva, B. et al. Atacama desert soil microbiology. In *Microbiology of Extreme Soils* (eds Dion, P. & Nautiyal, C. S.) 117–132 (Springer, Berlin, (2008).
31. Kebede, Martin, B., Nienhuis, J. & King, G. Leaf anatomy of two Lycopersicon species with contrasting gas exchange properties. *Crop Sci.* **34**, 108–113. <https://doi.org/10.2135/cropsci1994.0011183X003400010019x> (1994).
32. Pointing, S. B., Warren-Rhodes, K. A., Lacap, D. C., Rhodes, K. L. & McKay, C. P. Hypolithic community shifts occur as a result of liquid water availability along environmental gradients in China's hot and cold hyperarid deserts. *Environ. Microbiol.* **9**, 414–424. <https://doi.org/10.1111/j.1462-2920.2006.01153.x> (2007).
33. Evenari, M., Shanan, L. & Tadmor, N. *The Negev, the Challenge of a Desert*. (Harvard Univ. Press, 1971).
34. Ashbel, D. Frequency and distribution of dew in Palestine. *Geogr. Rev.* **39**, 291–297 (1949).
35. Oke, T. R. *Boundary Layer Climates*. (Wiley, 1978).
36. Kidron, G. J. The effect of substrate properties, size, position, sheltering and shading on dew: an experimental approach in the Negev Desert. *Atmos. Res.* **98**, 378–386. <https://doi.org/10.1016/j.atmosres.2010.07.015> (2010).
37. Beysens, D. The formation of dew. *Atmos. Res.* **39**, 215–237. [https://doi.org/10.1016/0169-8095\(95\)00015-J](https://doi.org/10.1016/0169-8095(95)00015-J) (1995).
38. Kidron, G. J. Wet-dry cycles on sandy and loessial Negev soils: implications for biocrust establishment and growth? *Ecohydrology* **15**, e2379. <https://doi.org/10.1002/eco.2379> (2022). Kronenfeld, R. Xiao, B. & Starinsky, A.
39. Kidron, G. J. & Kronenfeld, R. One year-long analysis: The contribution of dewfall and distillation to rock- and cobble-inhabiting lichens in the Negev. *Flora* **300**, 152240. <https://doi.org/10.1016/j.flora.2023.152240> (2023).
40. Kidron, G. J. A simple weighing method for dew and fog measurements. *Weather* **53**, 428–433. <https://doi.org/10.1002/j.1477-8696.1998.tb06362.x> (1998).
41. Beysens, D., Pruvost, V. & Pruvost, B. Dew observed on cars as proxy for quantitative measurements. *J. Arid Environ.* **135**, 90–95. <https://doi.org/10.1016/j.jaridenv.2016.08.014> (2016).
42. Jackson, R. D. Water vapor diffusion in relatively dry soil: II. Desorption experiments. *Soil. Sci. Soc. Am. J.* **28**, 464–466. <https://doi.org/10.2136/sssaj1964.03615995002800040006x> (1964).
43. Cary, J. W. Soil moisture transport due to thermal gradients: Practical aspects. *Soil. Sci. Soc. Am. J.* **30**, 428–433. <https://doi.org/10.2136/sssaj1966.03615995003000040011x> (1966).
44. Rose, C. W. Water transport in soil with daily temperature wave. I. Theory and experiment. *Aust J. Soil. Res.* **6**, 31–44 (1968a).
45. Rose, C. W. Water transport in soil with daily temperature wave. II. Analysis. *Aust J. Soil. Res.* **6**, 45–57 (1968b).
46. Phillip, J. R. & De Vries, D. A. Moisture movement in porous materials under temperature gradients. *Trans. Am. Geophys. Union* **38**, 222–232. <https://doi.org/10.1029/TR038i002p00222> (1957).
47. Hadas, A. Simultaneous flow of water and heat under periodic heat fluctuations. *Soil. Sci. Soc. Am. J.* **32**, 297–301. <https://doi.org/10.2136/sssaj1968.036159950032000300015x> (1968).

48. Cahill, A. T. & Parlange, M. B. On water transport in field soils. *Water Res. Res.* **34**, 731–739. <https://doi.org/10.1029/97WR03756> (1998).
49. Or, D. & Wraith, J. M. Comment on on water vapor transport in field soils by Anthony T. Cahill and Marc B. Parlange. *Water Resour. Res.* **36**, 3103–3105. <https://doi.org/10.1029/2000WR900124> (2000).
50. Zeng, Y. et al. Diurnal soil water dynamics in the shallow vadose zone (field site of China University of Geoscience, China). *Environ. Geol.* **58**, 11–23. <https://doi.org/10.1007/s00254-008-1485-8> (2009).
51. Lu, S., Ren, T., Yu, Z. & Horon, R. A method to estimate the water vapour enhancement factor in soil. *Eur. J. Soil. Sci.* **62**, 498–504. <https://doi.org/10.1111/j.1365-2389.2011.01359.x> (2011).
52. Cary, J. W. Water flux in moist soil: thermal versus suction gradients. *Soil. Sci.* **100**, 168–175 (1965).
53. Cockell, C. S. & Stokes, M. D. Hypolithic colonization of opaque rocks in the Arctic and Antarctic polar deserts. *Arc Antarct Alp. Res.* **38**, 335–342 (2006).
54. Kidron, G. J. Analysis of dew precipitation in three habitats within a small arid drainage basin, Negev Highlands, Israel. *Atmos. Res.* **55**, 257–270. [https://doi.org/10.1016/S0169-8095\(00\)00063-6](https://doi.org/10.1016/S0169-8095(00)00063-6) (2000).
55. Chenu, C. Clay-or sand- polysaccharide associations as models for the interface between micro-organisms and soil: water related properties and microstructure. *Geoderma* **56**, 143–156 (1993).
56. Kidron, G. J. & Starinsky, A. Measurements and ecological implications of non-rainfall water in desert ecosystems – A review. *Ecohydrology*. <https://doi.org/10.1002/eco.2121> (2019). 12;e2121.
57. Kidron, G. J., Temina, M. & Starinsky, A. An investigation of the role of water (rain and dew) in controlling the growth form of lichens on cobbles in the Negev Desert. *Geomicrobiol. J.* **28**, 335–346. <https://doi.org/10.1080/01490451.2010.501707> (2011).
58. Kappen, L., Lange, O. L., Schulze, E. D., Evenari, M. & Buschbom, V. Ecophysiological investigations on lichens of the Negev Desert, IV: Annual course of the photosynthetic production of *Ramalina maciformis* (Del.) Bory. *Flora* **168**, 85–105. [https://doi.org/10.1016/S0367-2530-\(17\)31899-6](https://doi.org/10.1016/S0367-2530-(17)31899-6) (1979).
59. Kidron, G. J. et al. The effect of water source on niche partitioning of chlorolichens and cyanobacteria—Implications for resilience? *Planta* **258**, 8. <https://doi.org/10.1007/s00425-023-04165-5> (2023).
60. Lange, O. L., Green, T. G. A., Melzer, B., Meyer, A. & Zellner, H. Water relations and CO₂ exchange of the terrestrial lichen *Teloschistes capensis* in the Namib fog Desert: measurements during two seasons in the field and under controlled conditions. *Flora* **201**, 268–280. <https://doi.org/10.1016/j.flora.2005.08.003> (2006).
61. Kappen, L. & Valladares, F. Opportunistic growth and desiccation tolerance: The ecological success of poikilohydrous autotrophs. In *Handbook of Functional Plant Ecology*. (eds. Pugnaire, F.I., Valladares, F.), 9–80 (Marcel Dekker, New York, 1974).
62. Wierczos, J. et al. Microbial colonization of Ca-sulfate crusts in the hyperarid core of the Atacama Desert: Implications for the search of life on Mars. *Geobiology* **9**, 44–60. <https://doi.org/10.1111/j.1472-4669.2010.00254.x> (2011).
63. Rosenan, N. & Gilad, M. Meteorological data. Atlas of Israel (Carta, Jerusalem, (1985).
64. Bitan, A. & Rubin, S. *Climatic Atlas of Israel for Physical and Environmental Planning and Design* (Ramat Publishing, 1991).
65. Evenari, M. Ecology of the Negev Desert, a critical review of our knowledge. In *Developments in Arid Zone Ecology and Environmental Quality* (ed Shuval, H.) 1–33 (Balaban ISS, Philadelphia, Pa, (1981).
66. Wetzel, R. G. & Westlake, D. F. Periphyton. In *A Manual on Methods for Measuring Primary Production in Aquatic Environments*. (ed. Vollenweider, R.A.), 33–40 Blackwell Scientific Pub. Oxford Edinburgh, (1969).
67. Kidron, G. J., Vonshak, A., Dor, I., Barinova, S. & Abeliovich, A. Properties and spatial distribution of microbiotic crusts in the Negev Desert. *Catena* **82**, 92–101. <https://doi.org/10.1016/j.catena.2010.05.006> (2010).

Acknowledgements

The available access granted by the Israeli Meteorological Service to the Sede Boqer MET station is highly acknowledged. We would like to sincerely thank two anonymous reviewers for their excellent comments that substantially improved the outcome of our manuscript.

Author contributions

GJK- conceptualization, measurements, analysis, writing and editing; RK- measurements; BX- graphics, writing and editing, AB, CPM, DO.- writing and editing.

Declarations

Competing interests

The authors declare no competing interests.

Additional information

Supplementary Information The online version contains supplementary material available at <https://doi.org/10.1038/s41598-024-73555-w>.

Correspondence and requests for materials should be addressed to G.J.K. or D.O.

Reprints and permissions information is available at www.nature.com/reprints.

Publisher's note Springer Nature remains neutral with regard to jurisdictional claims in published maps and institutional affiliations.

Open Access This article is licensed under a Creative Commons Attribution-NonCommercial-NoDerivatives 4.0 International License, which permits any non-commercial use, sharing, distribution and reproduction in any medium or format, as long as you give appropriate credit to the original author(s) and the source, provide a link to the Creative Commons licence, and indicate if you modified the licensed material. You do not have permission under this licence to share adapted material derived from this article or parts of it. The images or other third party material in this article are included in the article's Creative Commons licence, unless indicated otherwise in a credit line to the material. If material is not included in the article's Creative Commons licence and your intended use is not permitted by statutory regulation or exceeds the permitted use, you will need to obtain permission directly from the copyright holder. To view a copy of this licence, visit <http://creativecommons.org/licenses/by-nc-nd/4.0/>.

© The Author(s) 2024